PROCEEDINGS OF SCIENCE

Critical behavior towards the chiral limit at vanishing and non-vanishing chemical potentials

Olaf Kaczmarek,[a] **Frithjof Karsch,**[a] **Anirban Lahiri,**[a] **Sheng-Tai Li,**[b] **Mugdha Sarkar,**[a,c,*] **Christian Schmidt**[a] **and Philipp Scior**[d]

[a] *Fakultät für Physik, Universität Bielefeld, Bielefeld, Germany*

[b] *Key Laboratory of Quark & Lepton Physics (MOE) and Institute of Particle Physics, Central China Normal University, Wuhan 430079, China*

[c] *Department of Physics, National Taiwan University, Taipei 10617, Taiwan*

[d] *Physics Department, Brookhaven National Laboratory, Upton, NY 11973, USA*

E-mail: okacz@physik.uni-bielefeld.de, karsch@physik.uni-bielefeld.de, alahiri@physik.uni-bielefeld.de, lishengtai@mails.ccnu.edu.cn, mugdha@physik.uni-bielefeld.de, schmidt@physik.uni-bielefeld.de, pscior@bnl.gov

We study the scaling behavior of the (2+1)-flavor QCD crossover region towards the chiral limit with smaller-than-physical light quark mass gauge ensembles, generated using the HISQ fermion discretization. At zero chemical potential, we study the fluctuations of conserved charges and their correlations with the chiral condensate, towards the chiral limit. We analyse the role of universal and regular contributions to the above quantities. We find a preliminary estimate of the leading curvature coefficient of the chiral phase transition line using scaling arguments.

The 38th International Symposium on Lattice Field Theory, LATTICE2021 26th-30th July, 2021 Zoom/Gather@Massachusetts Institute ofphysics Technology

*Speaker

PoS(LATTICE2021)429

1. Introduction

Knowledge of the nature of the chiral phase transition is a crucial piece of the puzzle of understanding the QCD phase diagram. With advances in high performance computing, lattice simulations with dynamical light quarks having smaller-than-physical masses have become feasible. This allows us to hunt for the signals of criticality towards the chiral limit, if any. A recent review of the motivations and the current developments of this field can be found in Ref. [1].

In the schematic 3d QCD phase diagram depicted in Fig. 1 (taken from Ref. [2]), we are interested in the chiral limit of the two degenerate light quarks ($m_{u,d} \equiv m_l = 0$) at vanishing chemical potential, which is accessible to lattice calculations. The chiral phase transition temperature T_c (denoted by the red dot in figure) was recently determined to be around 132 MeV [3], which is below the crossover temperature T_{pc} at physical quark masses [4, 5]. However, the order of the chiral phase transition is still not clear beyond doubt. Depending on the restoration of the anomalously broken $U_A(1)$ symmetry around T_c, one possibility is that the chiral phase transition is a second order transition belonging to the 3d O(4) universality class [6], which seems to be preferred from recent studies [3, 7–10] over other possibilities.

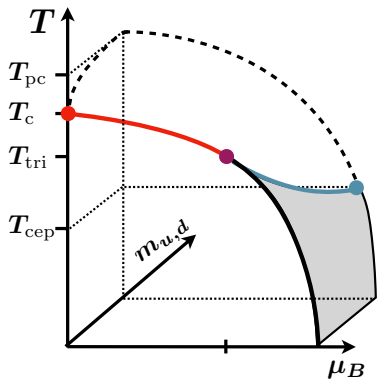

Figure 1: Schematic phase diagram for (2+1)-flavor QCD [2] in the temperature (T), baryon chemical potential (μ_B) and light quark mass (m_l) directions.

In this proceedings, we present our investigations of the conserved charge fluctuations calculated with smaller-than-physical light quark masses. The imprint of the criticality on these observables is important from the viewpoint of the heavy-ion collision experiments [11, 12]. We further report on mixed observables which are derivatives of the free energy density with respect to the light quark mass and chemical potential. Next, we present a preliminary calculation of the curvature of the chiral phase transition line at non-vanishing chemical potentials. The curvature in the chiral limit is important for locating the supposed tricritical point at $T = T_{\rm tri}$, denoted by the maroon dot at the end of the red second order transition line in Fig. 1. The tricritical point in turn affects the location of the critical endpoint $T_{\rm cep}$ [13] (denoted by the blue point in Fig. 1), which is being actively searched for in experiments.

2. Lattice setup

The gauge ensembles have been generated with HISQ fermion discretization and tree-level improved Symanzik gauge action. The ensembles were generated starting from physical light quark mass $m_l = m_s/27$ to smaller-than-physical light quark masses $m_l = m_s/40, m_s/80, m_s/160$, keeping strange quark mass m_s fixed at physical values, with corresponding pion masses of 140 MeV, 110 MeV, 80 MeV and 58 MeV. For scale setting, we use the kaon decay constant obtained in calculations with the HISQ action, i.e., $f_K = 156.1/\sqrt{2}$ MeV [14]. We present results from measurements done

at the largest simulated volumes for each mass at fixed time extent $N_\tau = 8$ with aspect ratios N_σ/N_τ in the range $4 - 7$.

3. Critical behavior of thermodynamic quantities

In Wilsonian RG theory, the couplings of the Hamiltonian near a fixed point in the infinite coupling space can be classified into those that respect the symmetry (which gets broken across the critical point) and those that break the symmetry explicitly. With respect to the chiral phase transition in hot and dense (2+1)-flavor QCD, the temperature T, chemical potentials μ_X for conserved charges $(X = B, Q, S)$, etc.[1], define the symmetry-preserving *energy-like* scaling field t and the light quark mass m_l defines the symmetry-breaking *magnetic-like* scaling field h. In the vicinity of the critical point, the dimensionless scaling fields are defined as

$$t = \frac{1}{t_0}\left(\frac{T - T_c}{T_c} + \kappa_2^X \left(\frac{\mu_X}{T}\right)^2\right), \qquad h \equiv \frac{H}{h_0} = \frac{1}{h_0}\frac{m_l}{m_s}, \tag{1}$$

where t_0, h_0 and κ_2^X are dimensionless non-universal constants and κ_2^X also denotes the leading order curvature of the chiral phase transition line.

Using the linearized approximation of the scaling fields near the critical point, we may express the free energy density f as the sum of singular (non-analytical) and regular contributions as [12],

$$\frac{f(t,h)}{T^4} = A h^{(2-\alpha)/\beta\delta} f_f(z) + \text{regular terms}, \tag{2}$$

where $f_f(z)$ is a universal scaling function of the scaling variable $z \equiv t/h^{1/\beta\delta}$, α, β and δ are the critical exponents of the universality class and A is a non-universal constant. With higher derivatives of f, the singular part becomes dominant and diverges in the chiral limit. The various scaling functions have been studied precisely for 3d O(2) [15] and O(4) [16] universality classes and have been successfully used to fit lattice data [7, 17, 18]. This indicates the possibility that the chiral phase transition belongs to the O(4) universality class. Since we work at finite lattice spacing with staggered quarks, we use 3d O(2) critical exponents in this study. Given the fact that the lattices used in this project are large enough [3], we use the infinite volume scaling functions in our analyses for any thermodynamic observable.

3.1 Fluctuations of conserved charges

We are interested in the behavior of conserved charge fluctuations at vanishing chemical potential as we move towards the chiral limit. From Eq. 2, the scaling behavior of the cumulants can be written as

$$\chi_{2n}^X \equiv -\frac{\partial^{2n} f/T^4}{\partial(\mu_X/T)^{2n}}\bigg|_{\mu_X=0} = -A_n (2\kappa_2^X)^n h^{(2-\alpha-n)/\beta\delta} f_f^{(n)}(z) + \text{regular terms}, \tag{3}$$

where $f_f^{(n)}(z)$ are derivatives of the universal free energy scaling function with respect to (w.r.t) z and A_n are non-universal constants. From Eq. 1, it is easy to show that two derivatives of f w.r.t

[1]The strange quark mass m_s may as well be considered to be an energy-like coupling as we shall do later.

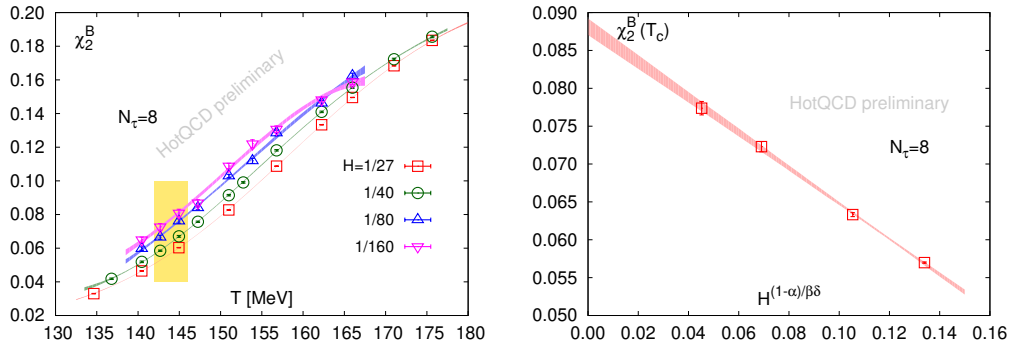

Figure 2: Left : The second order cumulant of baryon number fluctuations, χ_2^B, as a function of the temperature at various quark mass ratios $H = m_l/m_s$. Right : The values of χ_2^B at $T = T_c^{N_\tau=8}$ plotted against $H^{(1-\alpha)/\beta\delta} = H^{0.61}$ (using 3d O(2) critical exponents).

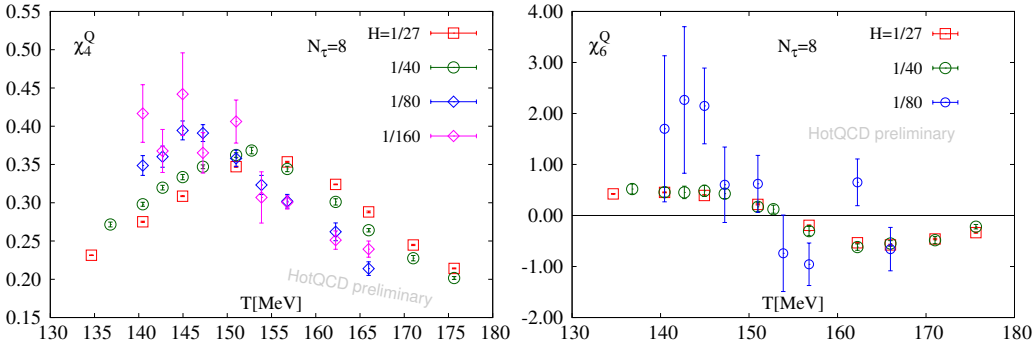

Figure 3: Left : The 4$^{\text{th}}$ order cumulant of electric charge fluctuations, χ_4^Q, as a function of the temperature for different H values. Right : The same as left but for the 6$^{\text{th}}$ order cumulant, χ_6^Q. The data for $H = 1/160$ is still too noisy.

μ_X yields the same singular part as a single derivative w.r.t T up to a constant. Hence, the $(2n)^{\text{th}}$ order cumulants are actually n^{th} order derivatives of f w.r.t T in terms of scaling behavior. For 3d O(N) models in general, α is negative and the divergence starts from 6$^{\text{th}}$ order onwards. The second order cumulants behave as the energy density and the fourth order cumulants behave as the specific heat which should develop a characteristic spike around T_c in the chiral limit [19]. We reported on this behavior in a previous proceeding [20]. Here we present the updated statistics in Figs 2 and 3.

The singular part of the second order cumulants at $T = T_c$ for different H could be estimated from a scaling fit which is linear in $H^{(1-\alpha)/\beta\delta}$, as can be seen from Eq. 3 and from the right-hand plot in Fig. 2. The ratios among the singular parts of different second order cumulants can be used to estimate the ratio of the curvatures along corresponding μ_X directions [20].

The features of the 4$^{\text{th}}$ and 6$^{\text{th}}$ order fluctuations are governed by the scaling functions $f_f''(z)$ and $f_f'''(z)$, respectively. These scaling functions for the 3d O(4) universality class can be found in Ref. [12]. We present updated results for the 4$^{\text{th}}$ and 6$^{\text{th}}$ order cumulants of the electric charge fluctuations in Fig. 3, where the improvement of the former one is vivid and the apparent increase in the peak height, according to the scaling expectation, can be better realized. Compared to Ref.

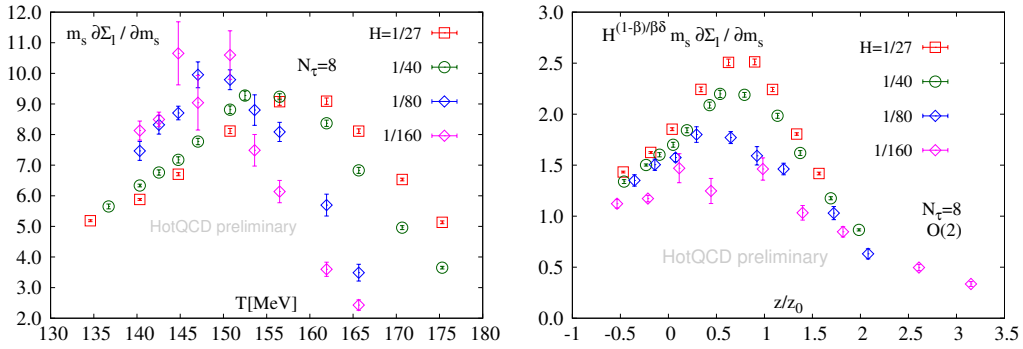

Figure 4: Left : The dimensionless strange mass m_s derivative of the light quark condensate Σ_l, $m_s\partial\Sigma_l/\partial m_s$, *versus* temperature for various H values. Right : The same quantity scaled by the factor $H^{(1-\beta)/\beta\delta}$ and plotted against $z/z_0 = H^{-1/\beta\delta}(T - T_c)/T_c$ for different H values.

[20], we have been able to add $H = 1/80$ data to the χ_6^Q calculation but it is evident that we still require more statistics.

3.2 Mixed observables

The mixed derivatives of the free energy density *i.e.* derivatives w.r.t both energy-like (t) and magnetic-like (h) couplings are divergent already from second order onward. We study two classes of mixed observables, corresponding to m_s derivatives of the light quark chiral condensate Σ_l, *i.e.* $m_s\partial\Sigma_l/\partial m_s$, and μ_X derivatives of Σ_l, *i.e.* $C_{2,X}^{\Sigma_l} \equiv \partial^2\Sigma_l/\partial\,(\mu_X/T)^2$, respectively. Since the strange mass m_s does not break the 2-flavor chiral symmetry, we consider it to be a energy-like coupling. The dimensionless light quark chiral condensate is defined in the f_K scale as

$$\Sigma_l = -\frac{m_s}{f_K^4}\frac{\partial f}{\partial m_l}\,. \tag{4}$$

Since we do not take the continuum limit in this work, we need not worry about the ultraviolet divergence in Σ_l. In terms of scaling behavior, Σ_l can be expressed as

$$\Sigma_l = h^{1/\delta} f_G(z) + \text{regular terms}\,, \tag{5}$$

where $f_G(z)$ is a universal scaling function related to $f_f(z)$ as $f_G(z) = -(1 + 1/\delta)f_f(z) + (z/\beta\delta)f_f'(z)$. Upon taking two derivatives w.r.t. μ_X, we have the following scaling expectation,

$$C_{2,X}^{\Sigma_l} = 2\kappa_2^X h^{(\beta-1)/\beta\delta} f_G'(z) + \text{regular terms}\,, \tag{6}$$

where the singular term is divergent for both $O(2)$ and $O(4)$ critical exponents. The mixed observable $m_s\partial\Sigma_l/\partial m_s$ has the same singular behavior up to a constant but with different regular contributions. It may be noted that $C_{2,X}^{\Sigma_l}$ is the leading order coefficient in the Taylor expansion of the light quark chiral condensate Σ_l in chemical potential μ_X. We refer to [4, 21] for the techniques used in the computation of Σ_l and its Taylor expansion coefficients.

We present our results for $m_s\partial\Sigma_l/\partial m_s$ and $C_{2,X}^{\Sigma_l}$ in the left panel of Fig. 4 and in Fig. 5, respectively. In the right plot of Fig. 4, we show $m_s\partial\Sigma_l/\partial m_s$ scaled by $H^{(1-\beta)/\beta\delta}$ plotted against

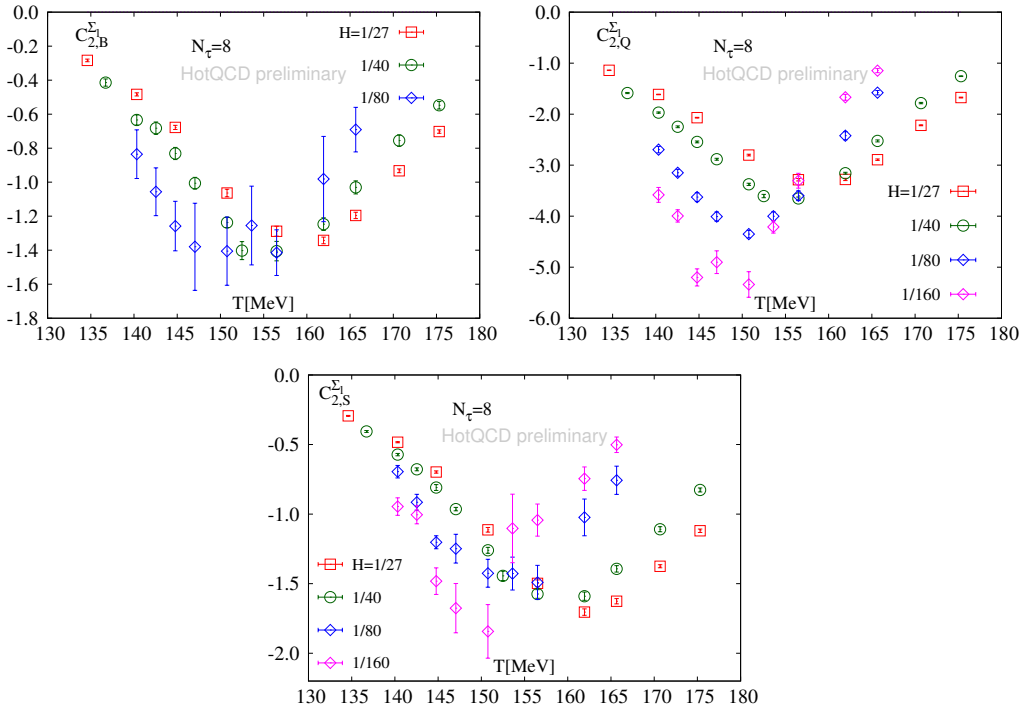

Figure 5: Top left : The second order Taylor coefficient, $C^{\Sigma_l}_{2,B}$, in the expansion of Σ_l around baryon number chemical potential $\mu_B = 0$, plotted against temperature at given H values. Top right : The same coefficient of the expansion in electric charge chemical potential μ_Q. Bottom : The same coefficient for strangeness chemical potential μ_S.

z/z_0. It can be easily seen from Eq. 6 that the scaled plot represents the scaling function $f'_G(z)$ up to a constant, in the absence of regular contributions. If we are close to the chiral limit, the regular terms would be negligible in comparison to the divergent singular part and we should observe the scaled data as a function of z/z_0 to fall on top of each other for different $H \to 0$. However, we do not observe such a behavior for our current H values in Fig. 4, which indicates that the regular contributions are not negligible. As discussed in Ref. [7], very similar observables w.r.t scaling expectation may behave quite differently in the lattice data, due to regular terms. We are currently investigating the role of various regular terms in our data. It should also be noted that we had presented results for some mixed observables in the T normalization previously [20], as opposed to f_K normalization in this proceeding. The change in normalization produces a qualitative change in the scaling behavior and we intend to discuss on this in more detail in a future study.

4. Curvature of the chiral phase transition line

From the definition of the reduced temperature t in Eq. 1, one can easily see that the condition $t(T, \mu_X) = 0$ maps out the chiral phase transition line in the $T - \mu_X$ plane. Using this condition, we can write the chiral transition temperature as a function of the chemical potential as

$$T_c(\mu_X) = T_c(0)\left(1 - \kappa_2^X \left(\frac{\mu_X}{T}\right)^2\right) . \tag{7}$$

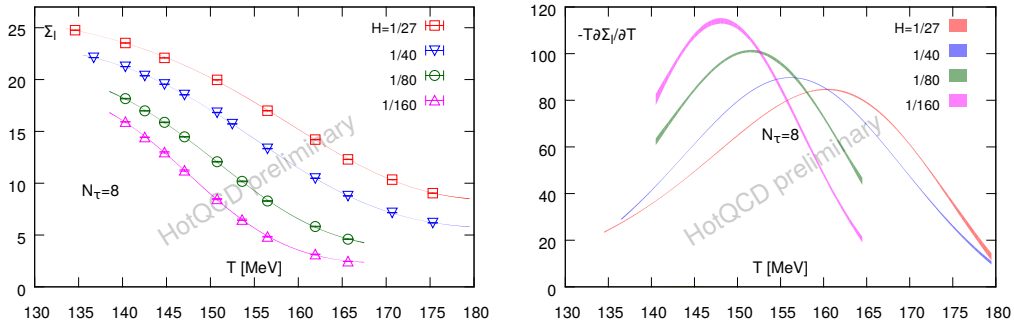

Figure 6: Left : The light quark chiral condensate Σ_l *versus* temperature, obtained at different H values. The data as a function of temperature has been interpolated using rational polynomials. Right : The temperature derivative, $-T\partial\Sigma_l/\partial T$, obtained from the fit of Σ_l shown in the left panel, is plotted against the temperature for various H values.

It is clear from the above that the coefficient κ_2^X determines the leading-order curvature of the chiral transition line for small μ_X values.

One can try to find an estimate of κ_2^X in the following way. For any observable O at $T = T_c$ and $\mu_X = 0$, we can rewrite the chemical potential and temperature derivatives, using Eq. 1, as,

$$\left.\frac{\partial^2 O}{\partial\left(\mu_X/T\right)^2}\right|_{(T_c,0)} = \frac{2\kappa_2^X}{t_0}\frac{\partial O}{\partial t}\,, \tag{8}$$

$$\left.\frac{\partial O}{\partial T}\right|_{(T_c,0)} = \frac{1}{t_0 T_c}\frac{\partial O}{\partial t}\,. \tag{9}$$

Combining Eqs. 8 and 9, we find an estimate for the chiral curvature at small values of chemical potential,

$$\kappa_2^X = \frac{T^2}{2T_c}\frac{\left(\partial^2 O/\partial\mu_X^2\right)\Big|_{(T_c,0)}}{\left(\partial O/\partial T\right)\Big|_{(T_c,0)}}\,. \tag{10}$$

At finite values of H, the derivatives of O may consist of regular contributions along with the singular part, which add corrections to κ_2^X. We choose O such that the singular parts diverge towards the chiral limit to obtain better estimates for κ_2^X from our data at small H values. One such choice is the chiral order parameter. We consider the light quark chiral condensate Σ_l in this discussion[2]. The scaling expectation of the μ_X derivative, $C_{2,X}^{\Sigma_l} \equiv \partial^2\Sigma_l/\partial\left(\mu_X/T\right)^2$, is given in Eq. 6. As discussed in Sec. 3.1, the T derivative of Σ_l should be the same as Eq. 6 except for factors of κ_2^X and different regular terms.

We already discussed our lattice results for $C_{2,X}^{\Sigma_l}$ at smaller-than-physical light quark masses in Fig. 5 in the previous section. To calculate the T derivative of Σ_l, we first interpolate Σ_l using rational polynomials, as shown in the left panel of Fig. 6, and then took the T derivative of the interpolating function to get $\partial\Sigma_l/\partial T$ which is shown in the right panel of Fig. 6. Finally, we

[2]We could have chosen instead the subtracted condensate Σ, but the presence of the strange quark condensate term may alter the singular behavior leading to non-trivial corrections in κ_2^X.

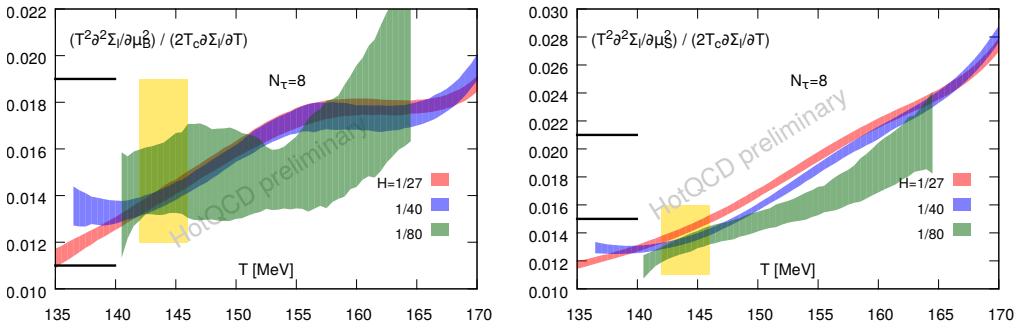

Figure 7: The ratio of the second order chemical potential derivative $\partial^2\Sigma_l/\partial\mu_X^2$ and temperature derivative $\partial\Sigma_l/\partial T$ of the light quark condensate Σ_l across the temperature range for various μ_X, $X = B, S$. The chiral limit estimates of κ_2^X get extracted in the yellow band around T_c. For comparison, we denote the 68% confidence interval of the continuum extrapolated results of the leading order curvature at physical mass, determined at T_{pc} for different μ_X [4], by black bars along the y-axis.

also interpolate the data of the μ_X derivatives and take the ratio of Figs. 5 and Fig. 6 to obtain the estimates of the curvature values shown in Fig. 7. The interpolations as well as the ratio calculation have been done on fake samples generated under Gaussian approximation with mean and standard deviation being the average and the uncertainty, respectively, of a particular data point. We read off the chiral curvature κ_2^X from the temperature interval around the chiral phase transition temperature on lattices with temporal extent $N_\tau = 8$, $T = T_c^{N_\tau=8} \simeq 144$ MeV (determined in Ref. [3]). The continuum extrapolated results for the curvature of the crossover line along various chemical potentials at physical masses [4] has been indicated by black bars in Fig. 7 (see figure caption). Our preliminary results suggest that the chiral limit result for the curvature coefficient κ_2^B remains almost unchanged from the physical mass curvature which may be argued from the relatively small change in the nucleon masses towards the chiral limit [22]. Similar calculation for μ_S is shown in the right panel of Fig. 7 and the corresponding chiral curvature coefficient κ_2^S at $N_\tau = 8$ appears to be below the corresponding continuum physical mass value. The curvature coefficient of the chiral transition line along various chemical potentials can also be obtained as a fit parameter from the scaling fit of the μ_X derivative of the chiral condensate with the ansatz given in Eq. 6. This has been tried in a previous work using the p4-action of staggered quarks [18] and we plan to repeat the same analysis with our current HISQ data. This will give a more complete picture about the mass dependence of the (pseudo-)critical lines towards the chiral limit.

The same ratio in Eq. 10, except for the factor $T^2/2T_c$ replaced by $T_{pc}/2$, was computed for thermodynamic observables like the pressure and energy density at physical mass $H = 1/27$ in Ref. [23]. The ratio represents the curvature of the line of constant physics (LCP) for the observables computed at $T = T_{pc}$ and $\mu_B = 0$. It was found that they agree quite well with the curvature of the crossover line along μ_B. From Fig. 7, we can also extract the curvature of the LCP of the chiral order parameter for $H = 1/27$ at $T = T_{pc}^{N_\tau=8} \simeq 161$ MeV and that seems to be in well agreement with previous determination of the curvature of the pseudo-critical line using various pseudo-critical conditions.

5. Conclusions and outlook

Our results at finite lattice spacing appear consistent with a chiral phase transition belonging to the 3d, O(2) universality class (3d, O(4) in the continuum). The scaling behavior of second order conserved charge fluctuations is similar to that of an energy density which allows us to separate the singular and regular contributions of these quantities at physical or any given masses. The ratios of the singular contributions provide an estimate of the ratio of the chiral limit curvatures, and it seems to indicate that the curvatures along various chemical potential directions depend weakly on the light quark mass. We expect the strange quark mass is an energy-like coupling w.r.t the 2-flavor chiral phase transition and the strange quark condensate to behave like an energy density. However, at our current H values, we need more detailed analyses including the regular contributions to understand the scaling behavior of the mixed observable, $m_s\partial\Sigma_l/\partial m_s$ better.

We provided a first preliminary result for the estimators of the curvature of the phase transition line in the chiral limit with the HISQ action. In agreement with the ratios of the curvatures from the second order cumulants, we find that the curvature changes only weakly as we move towards the chiral limit.

Next, we plan to do a scaling analysis with input from the previously known 3d, O(2) scaling functions to understand the interplay of the singular and regular contributions in the observables. In addition, the fluctuations at smaller-than-physical masses in the hadronic phase shall be compared to predictions from the HRG model, which by itself cannot capture the critical behavior. In the future, we plan to do an extensive study at different lattice spacings and volumes for different masses to take the chiral, continuum and thermodynamic limits.

Acknowledgements

This work was supported by the Deutsche Forschungsgemeinschaft (DFG, German Research Foundation) Proj. No. 315477589-TRR 211; and by the German Bundesministerium für Bildung und Forschung through Grant No. 05P18PBCA1. We thank the HotQCD for providing access to their latest data sets and for many rewarding discussions.

References

[1] A. Lahiri, *Aspects of finite temperature QCD towards the chiral limit*, in *38th International Symposium on Lattice Field Theory*, 12, 2021, 2112.08164.

[2] F. Karsch, *Critical behavior and net-charge fluctuations from lattice QCD*, *PoS* **CORFU2018** (2019) 163 [1905.03936].

[3] HotQCD collaboration, *Chiral Phase Transition Temperature in (2+1)-Flavor QCD*, *Phys. Rev. Lett.* **123** (2019) 062002 [1903.04801].

[4] HotQCD collaboration, *Chiral crossover in QCD at zero and non-zero chemical potentials*, *Phys. Lett. B* **795** (2019) 15 [1812.08235].

[5] S. Borsanyi, Z. Fodor, J. N. Guenther, R. Kara, S. D. Katz, P. Parotto et al., *QCD Crossover at Finite Chemical Potential from Lattice Simulations*, *Phys. Rev. Lett.* **125** (2020) 052001 [2002.02821].

[6] R. D. Pisarski and F. Wilczek, *Remarks on the Chiral Phase Transition in Chromodynamics*, *Phys. Rev. D* **29** (1984) 338.

[7] D. A. Clarke, O. Kaczmarek, F. Karsch, A. Lahiri and M. Sarkar, *Sensitivity of the Polyakov loop and related observables to chiral symmetry restoration*, *Phys. Rev. D* **103** (2021) L011501 [2008.11678].

[8] A. Bazavov et al., *Meson screening masses in (2+1)-flavor QCD*, *Phys. Rev. D* **100** (2019) 094510 [1908.09552].

[9] H. T. Ding, S. T. Li, S. Mukherjee, A. Tomiya, X. D. Wang and Y. Zhang, *Correlated Dirac Eigenvalues and Axial Anomaly in Chiral Symmetric QCD*, *Phys. Rev. Lett.* **126** (2021) 082001 [2010.14836].

[10] F. Cuteri, O. Philipsen and A. Sciarra, *On the order of the QCD chiral phase transition for different numbers of quark flavours*, *JHEP* **11** (2021) 141 [2107.12739].

[11] S. Ejiri, F. Karsch and K. Redlich, *Hadronic fluctuations at the QCD phase transition*, *Phys. Lett. B* **633** (2006) 275 [hep-ph/0509051].

[12] B. Friman, F. Karsch, K. Redlich and V. Skokov, *Fluctuations as probe of the QCD phase transition and freeze-out in heavy ion collisions at LHC and RHIC*, *Eur. Phys. J. C* **71** (2011) 1694 [1103.3511].

[13] Y. Hatta and T. Ikeda, *Universality, the QCD critical / tricritical point and the quark number susceptibility*, *Phys. Rev. D* **67** (2003) 014028 [hep-ph/0210284].

[14] A. Bazavov et al. [MILC collaboration], *Results for light pseudoscalar mesons*, *PoS(LATTICE2010)* (2010) 074 [1012.0868].

[15] J. Engels, S. Holtmann, T. Mendes and T. Schulze, *Equation of state and Goldstone mode effects of the three-dimensional O(2) model*, *Phys. Lett. B* **492** (2000) 219 [hep-lat/0006023].

[16] J. Engels and F. Karsch, *The scaling functions of the free energy density and its derivatives for the 3d O(4) model*, *Phys. Rev. D* **85** (2012) 094506 [1105.0584].

[17] S. Ejiri, F. Karsch, E. Laermann, C. Miao, S. Mukherjee, P. Petreczky et al., *On the magnetic equation of state in (2+1)-flavor QCD*, *Phys. Rev. D* **80** (2009) 094505 [0909.5122].

[18] O. Kaczmarek, F. Karsch, E. Laermann, C. Miao, S. Mukherjee, P. Petreczky et al., *Phase boundary for the chiral transition in (2+1) -flavor QCD at small values of the chemical potential*, *Phys. Rev. D* **83** (2011) 014504 [1011.3130].

[19] A. Cucchieri, J. Engels, S. Holtmann, T. Mendes and T. Schulze, *Universal amplitude ratios from numerical studies of the three-dimensional O(2) model*, *J. Phys. A* **35** (2002) 6517 [cond-mat/0202017].

[20] M. Sarkar, O. Kaczmarek, F. Karsch, A. Lahiri and C. Schmidt, *Conserved charge fluctuations in the chiral limit*, *Acta Phys. Polon. Supp.* **14** (2021) 383 [2011.00240].

[21] P. Steinbrecher, *The QCD crossover up to $O(\mu_B^6)$ from Lattice QCD*, Ph.D. thesis, U. Bielefeld (Germany), 2018, https://pub.uni-bielefeld.de/record/2919977.

[22] R. D. Young and A. W. Thomas, *Octet baryon masses and sigma terms from an SU(3) chiral extrapolation*, *Phys. Rev. D* **81** (2010) 014503 [0901.3310].

[23] A. Bazavov et al., *The QCD Equation of State to $O(\mu_B^6)$ from Lattice QCD*, *Phys. Rev. D* **95** (2017) 054504 [1701.04325].

PoS(LATTICE2021)429